Allocca, C., Chen, Q., and Glicksman, L.R. 2003. "Design analysis of single-sided natural ventilation," Energy and Buildings, *35(8), 785-795.*

Design analysis of single-sided natural ventilation

Camille Allocca[1], Qingyan Chen[2,*], and Leon R. Glicksman[1]

Building Technology Program, Massachusetts Institute of Technology,
Room 5-418, 77 Massachusetts Avenue, Cambridge, MA 02139-4307, USA

School of Mechanical Engineering, Purdue University
585 Purdue Mall, West Lafayette, IN 47907-2040, USA

Abstract

Natural ventilation is an effective measure to save energy consumed in buildings and to improve indoor air quality. This investigation studied single-sided natural ventilation by using a computational fluid dynamics (CFD) model, together with analytical and empirical models. The CFD model was applied to determine the effects of buoyancy, wind, or their combination on ventilation rates and indoor conditions. For buoyancy-driven flow, the CFD results are within a 10% difference from the semi-analytical results. For combined wind- and buoyancy-driven flow, CFD may have under predicted the empirical model results by approximately 25%. This investigation also studied the effects of opposing buoyancy and wind forces.

Keywords: Natural ventilation; CFD; analytical method

1. Introduction

Sustainable development in the building industry requires designers to satisfy the needs of today's users without compromising the ability of future generations to meet their own needs. Mechanical ventilation and air conditioning of buildings consume large amounts of energy in the world, especially in developed countries, where buildings are responsible for one third of all energy consumption [1]. This increased use of mostly fossil-based energy leads to atmospheric pollution and global warming. Natural ventilation is an energy efficient alternative for reducing the energy use in buildings, achieving thermal comfort, and maintaining a healthy indoor environment [2,3,4]. Typically, the energy cost of a naturally ventilated building is 40% less than that of an air-conditioned building [5]. Natural ventilation, therefore, contributes to a sustainable environment by reducing energy use in buildings. Natural ventilation has become a new trend in building design in architectural community [6,7] and has been used in many types of buildings, even in highly indoor climate controlled hospitals [8]. However, it should be pointed out that natural ventilation can only be applied to certain climates and it has many limitations [9]. Even local noise and pollution level would limits the applications of natural ventilation. Many of the past studies on natural ventilation were limited to a certain components, such as its driving force [10,11], or some of the mechanism [12], or a simple one-story building [13] There are two main types of natural ventilation: cross and single-sided ventilation. In the U.S., large and thick building shapes, fire codes, security requirements, and privacy concerns often prevent the design of

* Corresponding author. Tel.: +1-765-496-7562, Fax: +1-765-496-7534, email address: yanchen@purdue.edu (Q.Chen).

cross ventilation. Single-sided ventilation is more acceptable than cross ventilation, despite its lower efficiency. Our focus is on single-sided ventilation.

The driving forces for natural ventilation are wind and buoyancy. Differences in wind pressure along the façade and differences between indoor and outdoor temperatures create a natural air exchange between indoor and outdoor air. The ventilation rate depends on the strength and direction of these forces and the resistance of the flow path. These physical processes are complex, and predicting ventilation rates is difficult. Hence, it is challenging to control natural ventilation in order to obtain the required indoor environment conditions. Most designs for single-sided ventilation focus on the effects of buoyancy-driven flow. There is a particular lack of information on the combined effects of wind and buoyancy on single-sided ventilation. It is important to fully understand and analyze single-sided natural ventilation under combined wind and buoyancy effects in order to make its design more effective. This paper reports our efforts in providing such information to designers.

2. Types of Single-Sided Natural Ventilation

The temperature difference across the opening(s) between an indoor and outdoor space and the wind forces are the two major parameters affecting airflow in single-sided natural ventilation. This section discusses how the two parameters create different types of single-sided natural ventilation.

2.1 Buoyancy-driven flow

For a space with a large opening or an upper and lower opening, a temperature difference between the indoor space and the outdoor environment causes a density difference, where the warm air is less dense than the colder air. As a result, a pressure difference occurs between the inside and outside air, as shown in Fig. 1(a). The higher internal pressure at the upper opening drives outflow and the lower internal pressure at the bottom opening drives inflow. This buoyancy-driven flow is also known as *stack* effect. As inside and outside temperatures equalize, the stack pressure approaches zero and there is no driving force for ventilation.

The location of ventilation openings determines the temperature distribution within a space. If two vents are open, one at the top of the space and the other at the bottom, cool air will flow into the lower opening, and warm air will flow out of the upper opening, as shown in Fig. 1(b). This type of ventilation, which creates a temperature stratification within the space, is sometimes called displacement ventilation. Although it has a much stronger effect for spaces with upper and lower openings, displacement ventilation can also occur in spaces with a single large opening, as shown in Fig. 1(c). In this case, the opening serves as both an air inlet and outlet. Compared with upper and lower openings, single openings generate lower ventilation rates and the ventilated air does not penetrate as far into the space. Stronger airflow will be induced when there is a large vertical separation between inlets and outlets, and when there is a large difference between indoor and outdoor temperatures.

2.2 Wind-driven flow

Single-sided natural ventilation can also be created by the pressure differences across a space's openings due to wind. The related physical processes are complex, because of the variability in wind conditions. Experimental results have shown that the fluctuating effects of the wind, attributed to the turbulent characteristics of the incoming wind and/or to turbulence induced by the building itself [14], are also responsible for single-sided ventilation.

Turbulence in the airflow along an opening causes simultaneous positive and negative pressure fluctuations of the inside air.

2.3 Combined buoyancy and wind-driven flow

In most cases, buoyancy-driven and wind-driven flows exist simultaneously. The simultaneous influence of temperature and wind on the ventilation process at an open window is very complicated because wind and stack forces reinforce or counteract each other.

Since wind-driven flow has been extensively studied, this investigation focuses on single-sided natural ventilation due to buoyancy-driven flow and combined wind- and buoyancy-driven flow, with the objective being to identify effective design tools for designers. The following section introduces the research methods used in this investigation.

3. Research Methods

Investigation of the complex flows of single-sided ventilation can be accomplished through analytical, experimental, and numerical studies.

3.1 Analytical methods

In order to study airflow parameters, various analytical methods have been developed. One such method, described in this section, involves applying simple equations from Bernoulli theory for buoyancy-driven flow, together with an empirical discharge coefficient, to single-sided ventilation.

The most important parameter for natural ventilation design is the volume flow rate through the opening(s). For single-sided ventilation through an upper and lower opening (Fig. 1(b)) of equal area, A, the volume flow rate through each opening is approximated as

$$\dot{V} = C_d A \sqrt{gh \frac{\Delta T}{T_{out}}} \tag{1}$$

where h is the height between the center of the openings and C_d is taken to be the discharge coefficient (equal to 0.6 for a doorway), which accounts for viscous losses at the area contraction [15]. This equation is valid when the difference between the outside and the average inside temperature, ΔT, is not large (<10°C) [15].

For a single large opening (Fig. 1(c)), the volume flow rate is

$$\dot{V} = \frac{C_d A}{3} \sqrt{gh \frac{\Delta T}{T_{out}}} \tag{2}$$

where h is the height of the window [16]. Since this airflow profile varies significantly along the opening height (see Fig. 1(c)), the airflow is integrated over this height, producing the 1/3 constant in this equation [16].

Since the analytical calculations assume a constant indoor air temperature, indoor temperature stratification and varying air density are neglected. Several complex models have been developed which more accurately represent the behavior of openings with temperature stratification. Li and his coworkers [17,18], for example, presents a series analytical models

with many assumptions on temperature profile. Nevertheless, these analytical methods are still limited in their applicability.

3.2 Experimental methods

Experimental results are valuable in determining how a specific physical process behaves. The measurements obtained from experimental methods can then be used to derive more general analytical models. Cockroft and Robertson [19] studied wind-driven ventilation through a single opening subjected to a turbulent impinging air stream, neglecting buoyancy effects. They derived a simple theoretical wind model to predict this type of airflow. The model was then compared with experiments from a large-scale model. The results from this study, however, only provided an indication of the magnitudes of airflows that wind may generate and concluded that further analysis and experiments were needed. Dascalaki et al. [20] also performed a wind-driven study, deriving the average airflow rate through the opening of single-sided natural ventilation configurations using tracer gas techniques. Carey and Etheridge [21] used a wind tunnel to study natural ventilation.

Most of the experimental methods have been applied to analyze the physical mechanisms of either buoyancy-driven or wind-driven flow through openings. One particularly detailed study analyzing the effects of both wind and temperature, separately and combined, has been performed by Phaff and deGids [22] to develop an empirical model. They conducted experiments on the lowest-floor apartments of three buildings in different locations, using tracer gas techniques, to measure the influence of wind and buoyancy on ventilation rates through a large opening. With the results, they created an empirical model, which quantified the combined effects of wind, temperature, and turbulence for single-sided ventilation. To represent natural ventilation provided in the absence of both wind and buoyancy, a constant turbulence term was added to the volume flow rate. This constant turbulence term is unique to this research study, as other studies on this subject make mention of only wind and buoyancy terms. The effect of turbulence was quantified by observed fluctuations in the air speed values. The resulting empirical model calculates an effective velocity, v_{eff}, through half the window opening, which is derived directly from the measured volume flow rate, $\dot{V}_{total}$.

$$v_{eff} = \frac{\dot{V}_{total}}{A/2} = \sqrt{\frac{2}{g}\left(\Delta p_{wind} + \Delta p_{stack} + \Delta p_{turbulence}\right)} = \sqrt{C_1 V_{met}{}^2 + C_2 h\Delta T + C_3} \quad (3)$$

where V_{met} is the meteorological wind speed, h is the vertical height of the opening, C_1 is a wind speed constant, C_2 is a buoyancy constant, and C_3 is a turbulence constant [22]. A reasonable correspondence between measured and calculated values was obtained for the fitting parameters, C_1=0.001, C_2=0.0035, and C_3=0.01 [22], yielding

$$v_{eff} = \frac{\dot{V}_{total}}{A/2} = \sqrt{0.001 \cdot V_{met}{}^2 + 0.0035 \cdot h\Delta T + 0.01} \quad (4)$$

The resulting empirical model closely fits the experimental data.

Phaff and deGids used meteorological data instead of locally measured data in order to fit the data from the different experimental locations with a single correlation. The problem with this approach is that this empirical equation in only applicable to the environment density types of the experiment (e.g. city, urban, rural, and country).

Note that the experimental methods can only deal with simple cases of flow since it is difficult to significantly change the design of an experimental setup. The value of the experimental method is therefore limited to the evaluation and analysis of existing structures. However, other methods, such as numerical modeling, are valuable in optimizing the various natural ventilation parameters during a building design.

3.3 Numerical methods

The last research method uses numerical techniques, such as computational fluid dynamics (CFD), which allows for the modeling of a wider array of flow phenomena, ranging from simple to complex cases. Since the method uses models to simulate turbulent flow, this leads to some uncertainties and requires model validation with experimental studies in order to have full confidence in the results.

CFD numerically solves the conservation equations of mass, momentum, and energy of flow. Because most indoor and outdoor airflows are turbulent, large eddy simulation and Reynolds averaged Navier-Stockes equations (RANS) with turbulence modeling can be used. Large eddy simulation is very promising and information, but it costs too much computing time for design purpose [23]. RANS with turbulence modeling links the unknown Reynolds-stresses to the mean flow variable through approximations (turbulence models). This type of turbulence modeling has been used a lot in the many studies concerning natural ventilation, such as [20,24]. There are many turbulence models that could be used in RANS. Chen [25, 26] studied various indoor airflows with eight different turbulence models and concluded that the Re-normalization Group (RNG) k-ε model [27] performed best. CFD solves the equations by discretizing them through the use of finite volume techniques that convert the flow-governing equations to a set of numerically solvable algebraic equations.

Several CFD studies have been performed for single-sided ventilation to study the effects of buoyancy-driven flow through a large opening. Schaelin et al. [28] simulated the bi-directional wind and stack flow through a door opening by coupling the indoor airflow to the outdoor flow. Li and Teh [29] did a similar study on stack flow alone. They found that the airflow rate increased with the power of the heat source and height of the window. Gan [30] evaluated the effective depth of fresh air in a particular space for buoyancy-driven flow through a large opening. However, those studies are purely numerical and do not compare results with analytical or experimental results. Although some of the studies have compared with experimental data, such as [24], the data was only temperature.

In addition, some of the past CFD studies on single-sided ventilation were performed for coupled outdoor and indoor flow and used an enlarged computational domain, while others assumed the flow domain to be the indoor environment itself. Perhaps the most important consideration is the selection of boundary conditions, which can have a major impact on the results. Therefore, it is necessary to validate CFD results and to conduct more CFD studies on boundary conditions.

Nevertheless, the CFD modeling has shown a great potential in the design stage. With the CFD results, designers decide optimum layouts and openings for the best natural ventilation. In addition, computational costs are decreasing while labor and material costs for experiments are increasing. Therefore, CFD modeling has become more and more popular and attractive in the design community.

Based on the comparison and analysis of the different research methods, this investigation uses the CFD method to study the buoyancy effect and the combined effect of wind and buoyancy on single-sided ventilation. However, the analytical and experimental methods are also used as references to demonstrate their pros and cons.

4. Setup

The building studied is a student dormitory in Boston. Our focus was to evaluate single-sided ventilation for a typical room that is 4.7 m long, 2.9 m wide, and 2.8 m high. The general room model used throughout the study is shown in Fig. 2. The furniture within this room consisted of a bed, desk, closet, and bookcase. The heat sources were a computer (300 W), a TV set (300 W), and one occupant (100 W). Each of the convective and radiative components comprises approximately a half of the total heat. This was calculated by simultaneously solving for the radiative heat component, convective heat component, and surface temperature of each heat source. Each heat source was modeled as a convective heat component. The surrounding walls, ceiling, and floor absorbed the radiative heat component, and released this heat back to the room air by convection. This study did not include the solar gains, for purposes of the time-averaged ventilation study.

The window layout for the room consisted of an upper and lower window (0.4 m^2 each), as shown in Fig. 2. In order to also address the single opening geometry trends for single-sided ventilation, another part of the investigation analyzed single-sided ventilation with a single 0.65 m^2 window. A window of this dimension (rather than a 0.8 m^2 opening, which would be equal to the total upper and lower opening size and therefore comparable) was chosen for this study because an empirical model that has been developed for single openings was based on a window of this average size and this model will be compared with CFD results later on in the study.

The outdoor air temperature was maintained constant at 25.5°C, the average noon temperature for Boston in July [31]. The intention was to analyze the results for this fixed outdoor temperature, and then to apply these results to a range of outdoor temperature conditions to develop trends.

5. Results

5.1 Buoyancy-driven flow

CFD analysis was first performed for buoyancy-driven single-sided ventilation without wind. The CFD technique solves a set of partial differential equations for the conservation of mass, momentum, energy, and species concentrations. These equations govern the transport phenomena in the indoor auto-racing complex. Since airflow in the building complex is turbulent, the CFD technique used a turbulence model (the renormalized-group k-ε model from Yakhot et al. [27]) to reduce the computing costs. With the turbulence model, the airflow, temperature, and species concentration transport can be described by the following unsteady time-averaged Navier-Stokes equations:

$$\frac{\partial(\rho\Phi)}{\partial t} + \mathrm{div}(\rho V\Phi - \Gamma_{\Phi,\mathrm{eff}} \cdot \mathrm{grad}\Phi) = S_\Phi \qquad (1)$$

Where

ρ = air density
Φ = 1 for mass continuity
= V_j (j = 1, 2, 3) for three components of momentum
= k for turbulent energy
= ε for the dissipation rate of k
= T for energy transport
= C_i for contaminant concentration i

V = velocity vector
$\Gamma_{\Phi,eff}$ = effective diffusion coefficient
S_Φ = source term

The RNG k-ε turbulence model [27] was built within the commercial software program, PHOENICS [32], which was used for the present investigation. Simulations were run for both an indoor and combined indoor and outdoor environment to determine appropriate boundary conditions. A comparison was then made between the two boundary conditions and the semi-analytical equations for buoyancy-driven flow in order to determine the CFD model performance.

The first CFD analysis used a flow domain the same size as the room (the indoor stack model), shown in Fig. 2. The upper and lower windows in the room were modeled as outlets at zero pressure and zero gradients for other variables, such as velocity and temperature. Assuming a zero pressure at each implies that the outside hydrostatic pressure was neglected. The CFD simulation seemed to produce reasonable buoyancy-driven airflow patterns, with colder air entering the room at the lower opening and warmer air exiting the room at the upper opening, as shown in Fig. 3(a). The temperature distribution (Fig. 3(b)) exhibited typical stratification characteristics for this form of ventilation. The air temperature in the room for this particular thermal conditions is higher than that for thermal comfort. However, over the entire summer period, we found that the temperature in the room is acceptable. For very hot summer conditions, such as the one shown in Fig. 3, auxiliary mechanical cooling may be necessary.

The second case included the outdoor environment as a combined model. The extension of the flow domain to the outdoor environment allows us to consider the vertical (hydrostatic) pressure distribution. This case also stacked three identical dormitory rooms vertically above one another to evaluate the effect along a building's height. This three-story setup was placed within a larger outside domain (see Fig. 4). This study found that the minimum dimension for the outer domain should be 10 m long (~2L), 6 m wide (~2W), and 12 m high (~1.5H), for which the results were independent of domain size. Since the convergence for buoyancy problems typically takes five to ten times longer than that for wind problems [33], it is necessary to minimize the computational domain of the stack model.

CFD is particularly sensitive to boundary conditions for buoyancy-driven flow. Unrealistically high airflows and unreasonable pressure distributions were found for the combined model when zero pressure boundary conditions were defined for the side and upper boundaries of the computational domain, i.e. the outside environment. Therefore, the present study used the following boundary conditions for the outside environment: solid plates with slip boundaries and a temperature equal to the outdoor air for all the side boundaries, zero-pressure boundary at the outdoor air temperature for the upper boundary, and solid adiabatic plate with non-slip boundary for the lower boundary. Fig. 5 shows that the velocity airflow field resulted in buoyancy-driven flow patterns similar to those of the indoor model. However, the magnitude of the overall velocity field was higher than that of the indoor model. Both the magnitudes and gradients for temperature also differed from those of the indoor model, with the combined model producing lower overall temperature values and gradients (see Fig. 6).

Although the spaces were physically and thermally isolated from one another, the temperatures in each space increased with height due to the outside thermal plume from the openings underneath, as shown in Fig. 6(a). This can clearly be seen from shifts in the graph of indoor temperature versus height shown in Fig. 6(b). This type of effect seems plausible for this case due to the small distance between upper openings of one space and lower openings of the above space. In reality, there is wind around the building and the wind can easily break down the thermal plumes. Nevertheless, the interaction of flows between the

vertical spaces cannot be ignored due to the very close proximity of the openings to each other in the case studied.

Both of the CFD models seemed to give reasonable flow patterns and exhibit temperature stratification characteristics. However, the ranges of values for the velocity and temperature fields were different from one another. In order to make a suitable comparison between these two models, the airflow rates were calculated and compared with the semi-analytical calculation (Eq. (1)). As illustrated in Table 1, Eq. (1) produced an airflow rate of 9.84 air changes per hour (ACH) at a ΔT of 2.83°C. This temperature difference of 2.83°C was not extracted from the CFD results but was calculated by solving both the semi-analytical airflow rate equation and an energy balance for the room simultaneously. The CFD simulations produced airflow rates of 5.42 ACH for the indoor stack model and 10.82 ACH for the combined indoor and outdoor stack model. The airflow rate for the combined model was taken at the lowest apartment, since semi-analytical calculations do not take into account the increasing shift in indoor temperature that has occurred in this situation. When compared with the semi-analytical calculation results, a 41% and 10% difference was found in the airflow rates for the indoor and combined models, respectively. The most important source of difference between the two model results was the choice of boundary conditions. These conditions dictated the flow patterns and temperature profiles within the space. The combined model took into account the outdoor hydrostatic pressure difference across the openings. These boundary conditions are more reasonable than the zero-pressure condition at all openings in the indoor stack model. The combined model therefore has a more solid physical background than the indoor stack only model. The airflow rate determined by this combined model produced consistent results when compared with the semi-analytical calculation. It is important to realize that the semi-analytical calculation assumed isothermal conditions within the room. This assumption is not appropriate for single-sided ventilation because thermal buoyancy relies on temperature stratification within the room to create air movement.

It should be noted the comparison in the case of the combined CFD model for a three-room building with the analytical calculation shown in Table 1 is only approximate. However, the one-room analytical model is actually used in practice for design natural ventilation in buildings with multiple stories. The comparison would nevertheless give designers a sense of possible errors introduced in their design.

In addition, although the spaces were physically and thermally isolated from one another, the temperatures in each space increased with height due to the outside thermal plume from the openings underneath, as was shown in Fig. 6. Although in reality the plume can be easily destroyed by wind, the indoor stack model and the semi-analytical equation cannot predict the impact of such a plume.

The combined indoor and outdoor flow model is therefore an appropriate tool for studying and designing single-sided ventilation with buoyancy-driven flow. This model is further used to study the impact of internal heat gains. In this extended study, the internal heat gains within the room were varied between 100 W and 1000 W with a break down of 60%/40% for radiative/convective components. These cases were simulated for both upper/lower and single opening geometries. For the single opening geometry cases, a 0.65 m wide and 1 m high window was modeled. These dimensions were the same as that used in the upcoming wind study, which reproduces a single-opening empirical model. The rest of the cases were the same as those with the two openings.

The airflow rate results from the combined indoor and outdoor flow model were compared with the semi-analytical equations (Eqs. (1) and (2)). The results for the upper and lower window and for the single window geometries for the lowest apartment are plotted in Fig. 7. The CFD results are again found to be within 10% of the semi-analytical solution

results. CFD has proven to be a reliable, valuable tool in analyzing buoyancy-driven single-sided ventilation over a range of conditions.

5.2 Combined wind and buoyancy driven flow

Although the study of purely buoyancy effects on single-sided ventilation is interesting, it is more useful to examine the effects of combined wind and buoyancy on the ventilation. Our intention is to use the empirical model of Phaff and deGids [22] so that we can evaluate CFD's ability for such a flow. In order to fit the parameters of the Phaff and deGids' experimental setup, the window in CFD was changed to a single opening and the window size was set to be the same as that in their study. The upper and lower opening room model shown in Fig. 8(a) was replaced with the single-opening room model shown in Fig. 8(b). Table 2 further compares the setup for the single opening CFD model and that of the three experimental cases. Since the room volume and floor area for the student residence case and that of the experiment are very similar, these parameters were not changed.

The CFD wind and stack model was based on the three-story apartment setup from the buoyancy-driven case (see Fig. 8), with an adjustment on the building aspect ratio to be the same as the real building. In order to ensure that the outer domain had no effect on the airflow around the building, the wind profile inlet was placed at 5 building heights (H) in front of and to either side of the building. The re-circulation zone for airflow around a three-dimensional block is reported to be approximately 5-7 times the height of the block [34]. Therefore, the outlet was safely placed at 10 building heights downwind of the building to ensure no disturbance of the flow. The upper boundary, placed at 4 building heights above the building, was found to have no effect on the airflow.

The CFD modeling was performed for various combinations of wind and stack effects. Meteorological wind speed was assumed to be in the range of 1-10 m/s. Since the experiments performed by Phaff and deGids took place in an urban environment, this appropriate wind profile was assumed to obey

$$V_h = 0.35 V_{met} h^{0.25} \tag{5}$$

where V_h is the local wind speed at height, h, and V_{met} is the meteorological wind speed (usually taken at 10m).

Since the empirical model was based on the experimental results from the lowest apartments of three buildings, our CFD analysis uses the results from the lowest apartment. Fig. 9 shows these CFD results compared with those of the Phaff and deGids model. In this figure, the results from The British Standards Code 5925 is also included [35]. This is a code of practice for natural ventilation design established by the British Standards Institution. In this standard, relationships for both wind and buoyancy-driven airflow through a large opening have also been developed. The results of the British Standards and Phaff and deGids are very similar, which in turn strengthens the validity of each of the model's cases. Both models are shown in Figure 9 as a basis for comparison. The CFD modeling is shown to underpredict the ventilation rates for the room by approximately 25% for velocities between 1 and 10 m/s. This may be due to the fact that RANS modeling in CFD solves for average airflow parameters rather than instantaneous airflow, which is believed to be a major component of the driving force for single-sided ventilation. Other computational studies in the literature have also found such a difference in their results [36].

This investigation has also used the CFD model to study combined wind and stack effect on single-sided ventilation through an upper and lower opening. The study was performed for a range of meteorological wind speeds of 1-10 m/s. Since the empirical models

of the British Standards and Phaff and deGids only account for a single opening geometry, the CFD results found for an upper and lower opening cannot be compared with empirical results. Nonetheless, these CFD results are also shown in Fig. 9. The ventilation rates for this window layout have greatly increased over those of a single opening. The same trend can be found for the buoyancy-driven flow according to the semi-analytical solutions.

Although experiments have found, for a particular tested room, that wind and stack flow reinforce each other according to the relationships in Eqs. (3) and (4), there is also evidence that wind and stack forces do not always reinforce each other, but in fact oppose each other. This ambiguity is illustrated in Fig. 10(a). An example of the counteracting wind and stack effect during an increasing progression of wind speeds is also shown in Fig. 10(b). In fact, a counteracting wind and stack flow did take place in the middle apartment of the CFD wind and stack model for both window geometry types. Fig. 11 shows the airflow at the mid-section in the room for an upper and lower opening. Velocity vectors were taken at a plane through the center of the middle apartment with meteorological wind speeds from 2-8 m/s. At a low 2 m/s wind speed, buoyancy effects were dominant and consequently drove air in through the lower opening and out through the upper opening. At a wind speed of 4 m/s, this buoyancy effect diminished as the wind-driven force through the upper opening increased. The buoyancy and wind forces were approximately equal at this wind speed, resulting in the minimum ventilation rate over the range of wind speeds given. As the wind speed increased to 6 m/s, the wind-driven force became dominant, thereby forcing a counterclockwise flow into the apartment, in through the upper opening and out through the lower opening. At 8 m/s, this wind force simply became stronger, with buoyancy effects becoming nearly negligible.

Unfortunately, there are no guiding rules to help in determining where the counteracting wind and stack effect would occur. Designers should be made aware of this physical phenomenon to better understand the characteristics of natural ventilation. In order to develop a set of rules for predicting this phenomenon, various different building sizes and shapes would need to be studied and modeled under different wind direction and speed. This is obviously not a trivial job. It may be more accurate to conduct CFD simulation than to use such a guide.

6. Conclusions

Various design features of single-sided ventilation have been explored and analyzed in order to gain a better understanding of the complexities and characteristics of this strategy. Based on results from analytical, empirical, and CFD models, trends were revealed and validated. Upon validation with analytical and empirical results, the CFD model is an appropriate tool for single-sided ventilation design and research.

For buoyancy-driven ventilation, the CFD model was very sensitive to how to set up the boundary conditions. The modeling requires the simulation of both the outdoor and indoor environment. With this effort, computed ventilation rates agree with the semi-analytical solutions with a less than 10% difference. It is not sufficient to limit the computational domain to only the indoor environment.

The CFD model was further applied to study combine effects of wind- and buoyancy-driven flow on single-sided natural ventilation over a range of wind speeds. The CFD results were compared with two empirical models from the literature, which were both based on a single opening setup for single-sided ventilation. The CFD model was found to follow the same trends as those empirical models, but consistently underestimate the ventilation rates by 25%.

This investigation also revealed that wind and stack effects may reinforce or oppose each other. This was verified by tracking the velocity patterns through a room at a range of wind speeds. No guiding rules could be established for predicting the occurrence of counteracting wind and stack effect, since no consistent trends were observed, but further research is recommended.

Acknowledgements

This work is supported by the U.S. National Science Foundation under grant CMS-9877118.

References

1. Energy Information Administration, State Energy Data Report 1995, Tables 3 through 7, 1995.
2. J.F. Busch, A Tale of Two Populations: Thermal comfort in air-conditioned and naturally ventilated offices in Thailand, Energy and Buildings 18 (3-4) (1992) 235-249.
3. R. Zhao, Y. Xia, Effective non-isothermal and intermittent air movement on human thermal responses, Roomvent 2 (1998) 351-357. 4. J.J. Finnegan, C.A.C. Pickering, P.S. Burge, The sick building syndrome: prevalence studies, British Medical Journal 289 (1994) 1573-1575.
4. J.J. Finnegan, C.A.C. Pickering, P.S. Burge, The sick building syndrome: prevalence studies, British Medical Journal 289 (1994) 1573-1575.
5. Energy Consumption Guide 19, Energy efficiency in offices, Energy Efficiency Office/HMSO, London, 1993.
6. A. Krishan, Climate responsive architecture: a design handbook for energy efficient buildings, Tata McGraw-Hill Pub. Co., New York, 2001.
7. T. Willmert, The return of natural ventilation, Architectural Record. 189(7), (2001): 137-148.
8. D. Clarke, A breath of fresh air, Hospital Development. 32(11), (2001): 13-17.
9. G.J. Levermore, The exponential limit to the cooling of buildings by natural ventilation, Building Services Engineering Research and Technology 23, no. 2 (2002): 119-125.
10. A.M. Rodrigues, A. Canha da Piedade, A. Lahellec, J.Y. Grandpeix, Modelling natural convection in a heated vertical channel for room ventilation, Building and Environment. 35, no. 5, (2000): 455-469.
11. J. Hirunlabh, S. Wachirapuwadon, N. Pratinthong, J. Khedari, New configurations of a roof solar collector maximizing natural ventilation, Building and Environment. 36, no. 3, (2001): 383-391.
12. D.W. Etheridge, Unsteady flow effects due to fluctuating wind pressures in natural ventilation design-instantaneous flow rates, Building and Environment. 35, no. 4, (2000): 321-337
13. G. Ziskind, V. Dubovsky, R. Letan, Ventilation by natural convection of a one-story building, Energy and Buildings. 34, (2002): 91.
14. F. Allard, Natural Ventilation in Buildings: A Design Handbook, James & James Ltd, London, 1998.
15. D. Etheridge, M. Sandberg, Building ventilation: Theory and measurement, John Wiley and Sons, Chichester, England, 1996.
16. H.B. Awbi, Air movement in naturally-ventilated buildings, Renewable Energy 8 (1996) 241-247.

17 Yuguo Li, Buoyancy-driven natural ventilation in a thermally stratified one-zone building, Building and Environment 35 (2000) 207-214.
18. Z.D. Chen, Z. D.and Y. Li. Buoyancy-driven displacement natural ventilation in a single-zone building with three-level openings, Building and Environment. 37, no. 3, (2002): 295-303.
19. J.P. Cockroft, P. Robertson, Ventilation of an enclosure through a single opening, Building and Environment 11 (1976) 29-35.
20. E. Dascalaki, M. Santamouris, A. Argiriou, C. Helmis, D.N. Asimakopoulos, On the combination of air velocity and flow measurements in single sided natural ventilation configurations, Energy and Building 24 (1996) 155-165.
21. P.S. Carey, D.W. Etheridge, Direct wind tunnel modelling of natural ventilation for design purposes, Building Services Engineering Research & Technology, 20, (1999): 131-140
22. J.C. Phaff, W.F.de Gids, J.A. Ton, D.V. van der Ree, L.L.M. Schijndel, The ventilation of buildings: Investigation of the consequences of opening one window on the internal climate of a room, Report C 448, TNO Institute for Environmental Hygiene and Health Technology (IMG-TNO), Delft, Netherlands, March 1980.
23. Y. Jiang and Q. Chen, Effect of fluctuating wind direction on cross natural ventilation in buildings from large eddy simulation, Building and Environment. 37, no. 4, (2002): 379-386
24. K.A. Papakonstantinou, C.T. Kiranoudis, N.C. Markatos Numerical simulation of air fow field in single-sided ventilated buildings, Energy and Buildings 33 (2000) 41-48.
25. Q. Chen, Comparison of different k-e models for indoor airflow computations, Numerical Heat Transfer 28 (B) (1995) 353-369.
26. Q. Chen, Prediction of room air motion by Reynolds-stress models, Building and Environment 31 (1996) 233-244.
27. V. Yakhot, S.A. Orzag, S. Thangam, T.B. Gatski, C.G. Speziak, Development of turbulence models for shear flows by a double expansion technique, Physics Fluids A 4 (1992) 1510-1520.
28. A.J. Schaelin, A. J. van der Maas, A. Moser, Simulation of Airflow through Large Openings in Buildings, ASHRAE Transactions 98 (1992) 319-328.
29. K. Li, S.L. Teh, Two-dimensional numerical study of airflow through large openings, Indoor Air 2 (1996) 1027-1032.
30. G. Gan, Effective depth of fresh air distribution in rooms with single-sided natural ventilation, Energy and Buildings 31 (2000) 65-73.
31. W. Marion, K. Urban, User's Manual for TMY 2 Typical Meteorological Years Derived from the 1961-1990 National Solar Radiation Data Base, June 1995.
32. CHAM, PHOENICS 3.1, CHAM Ltd., UK, 1999.
33. D. Bienfait, L. Vandaele, J. van der Maas, R. Walker, Single-sided ventilation, Proceedings of the 12th AIVC Annual Conference on Innovations in Ventilation Technology, Ottawa, Canada, 1991.
34. D.W. Etheridge, P.H. Kemp, Measurements of turbulent flow downstream of a rearward-facing step, Journal of Fluid Mechanics 86 (3) (1978) 545-566.
35. British Standards 5925: 1991, Code of practice for ventilation principles and designing for natural ventilation, British Standards Institute, 1991.
36. Muriel Regard-Alchakkif, Francois-Remi Carrie, Gerard Guarracino, Natural ventilation of a room through a large external opening: calculation using a CFD code, Rev Gen Therm, (in French) 37 (1997) 137-147.

Table 1
Comparison of air change rate (ACH) results for various models

Method	ACH	Percent Difference (%)
Semi-analytical calculation	9.84	(standard of comparison)
Indoor stack model	5.81	-41
Combined indoor and outdoor stack model (lowest apartment)	10.82	+10

Table 2
Comparison between experimental and CFD setup

Dimension	Experiment (values averaged for three spaces [22])	CFD Single Opening Model
Room volume (m^3)	38.0	38.2
Floor Area (m^2)	12.7	13.7
Window Area (m^2)	0.65	0.65

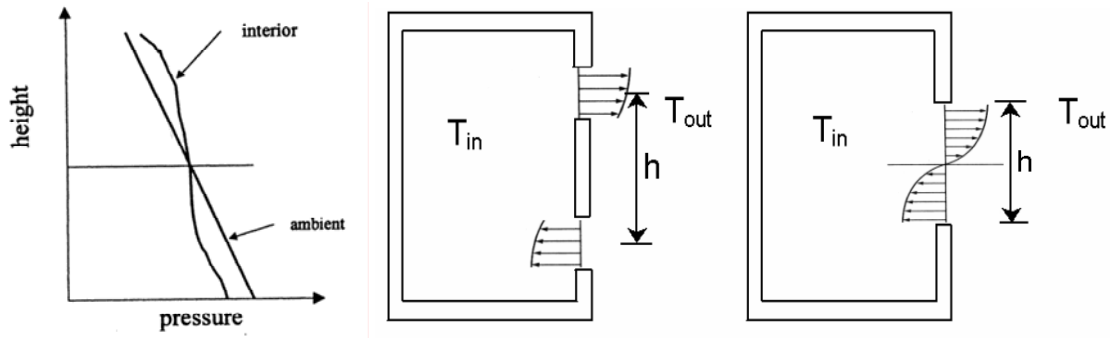

(a) (b) (c)

Fig. 1. Indoor and outdoor pressure distribution for buoyancy-driven flow (a) causing flow through an upper and lower opening (b) or a single opening (c).

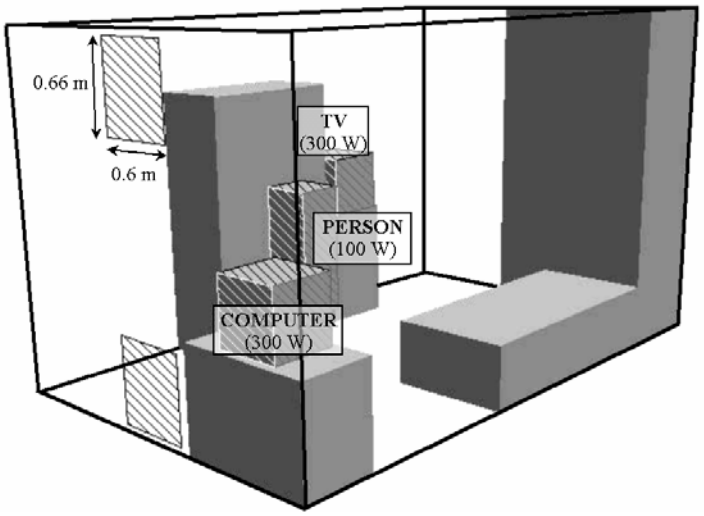

Fig. 2. Indoor stack model for single-sided ventilation study in CFD.

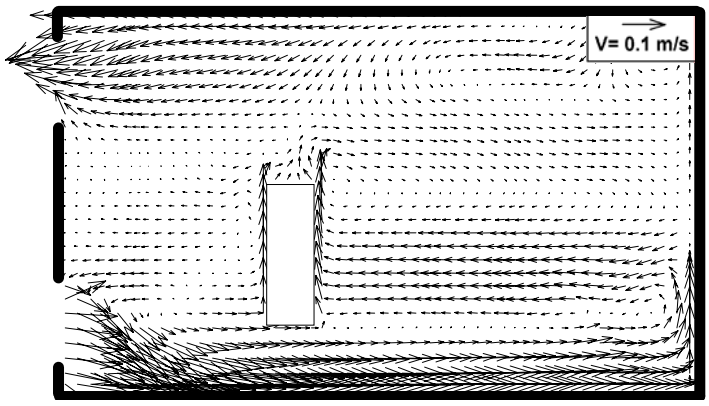

(a)

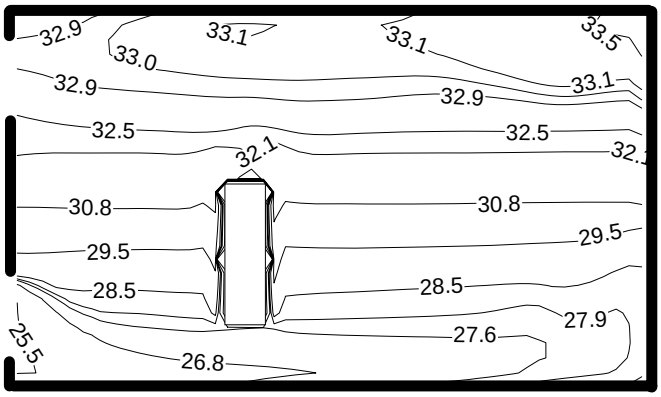

(b)

Fig. 3: CFD results for indoor stack model in the center section of the room: (a) velocity vectors and (b) temperature contours (°C)

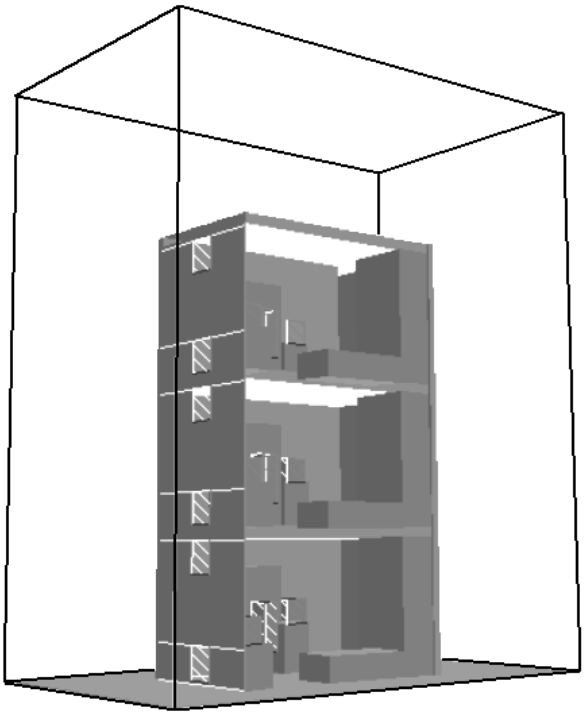

Fig. 4. Combined indoor and outdoor stack model for single-sided ventilation study in CFD.

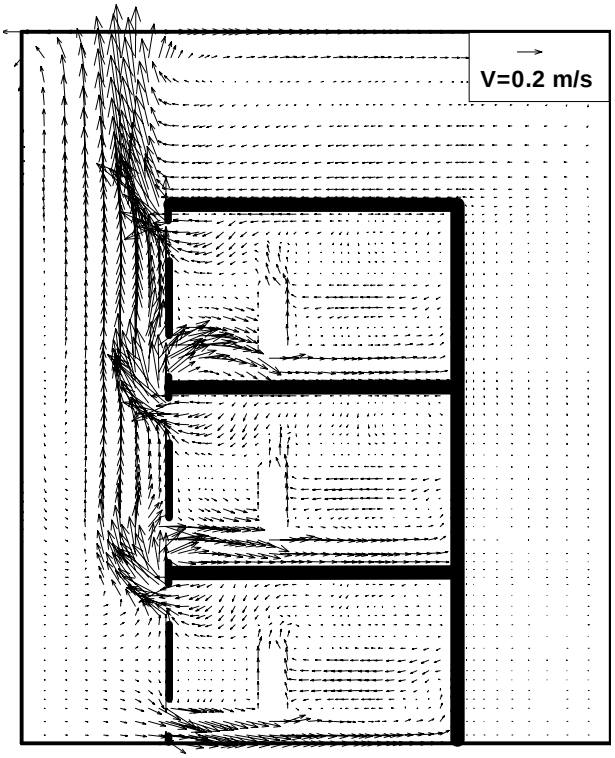

Fig. 5. Velocity vectors for combined model in the center of the rooms.

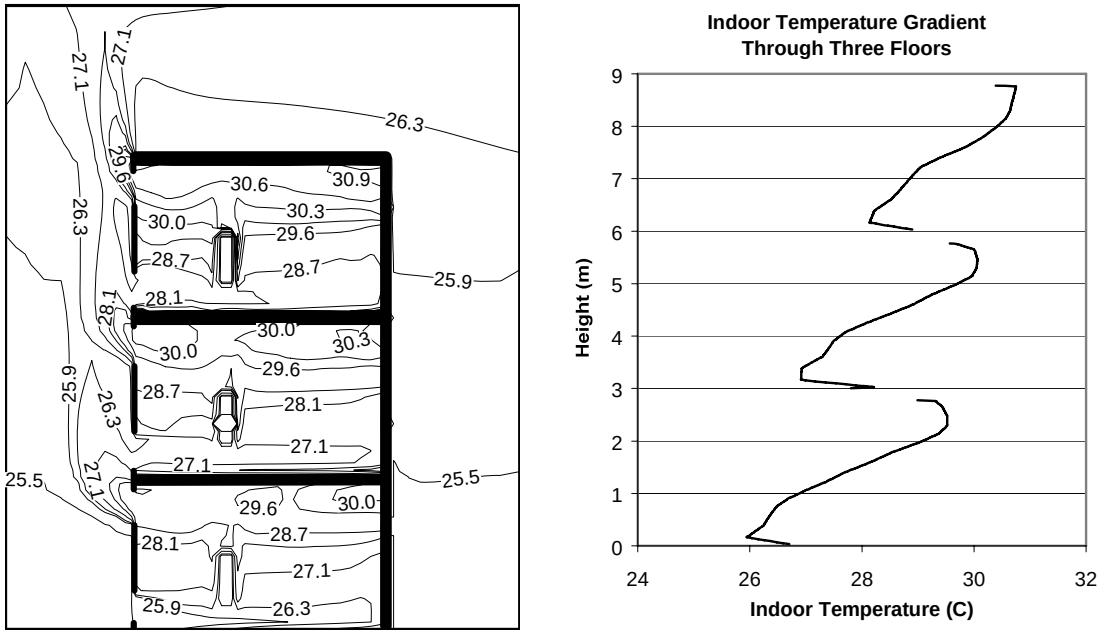

(a) (b)

Fig. 6. CFD results for the combined model in the center of the rooms: (a) temperature distribution and (b) vertical temperature profiles.

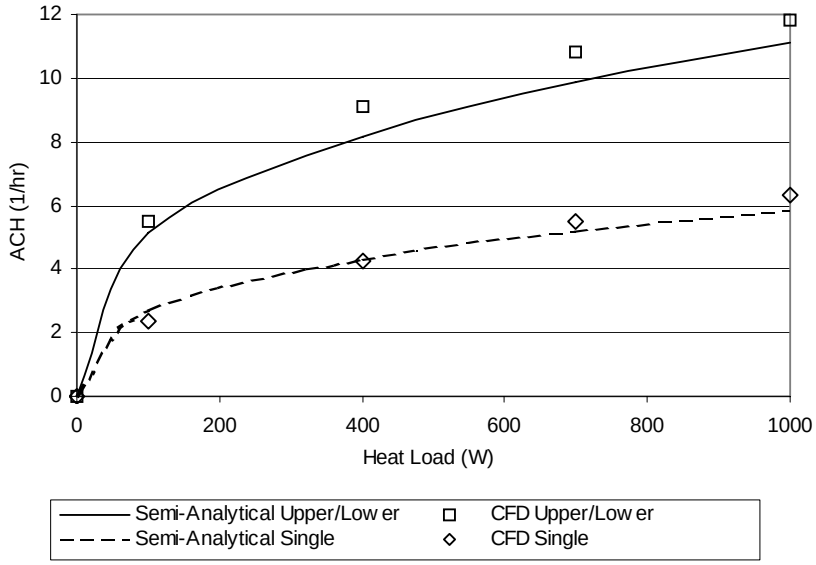

Fig. 7. Semi-analytical and computational (combined model - lowest apartment) air change rate (ACH) results over a range of internal heat loads for an upper and lower opening and single opening geometry.

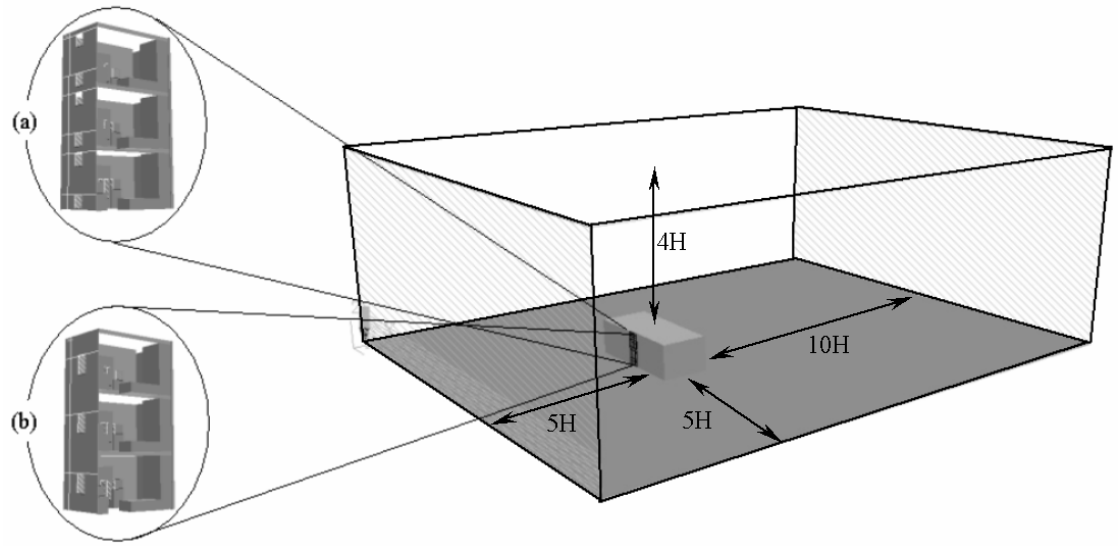

Fig. 8. CFD domain for wind and stack model: (a) upper/lower opening geometry and (b) single opening geometry; H=building height.

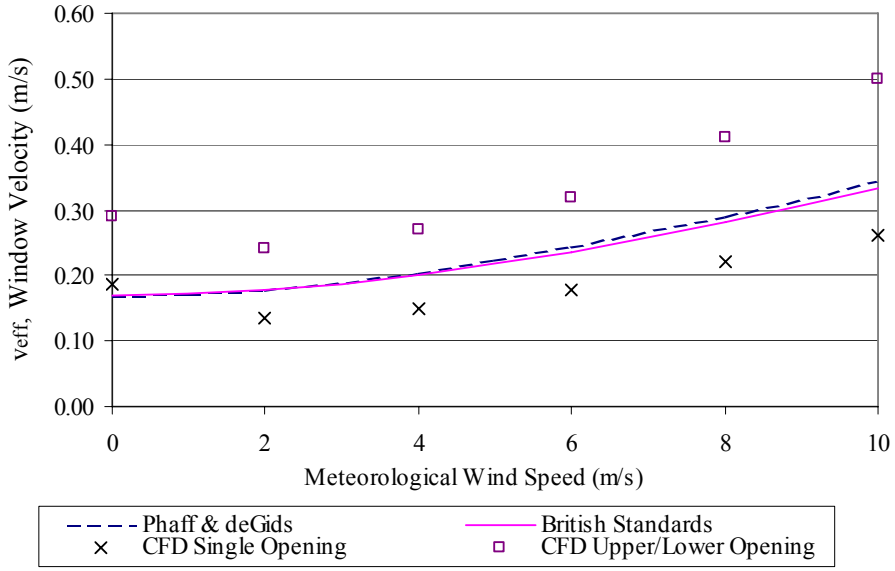

Fig. 9. Combined wind and buoyancy-driven ventilation rates through an upper and lower opening or a single opening: CFD results vs. empirical models.

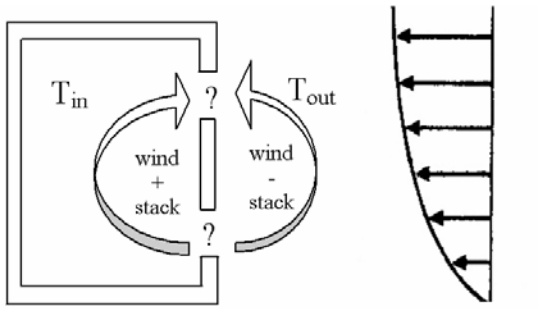

(a)

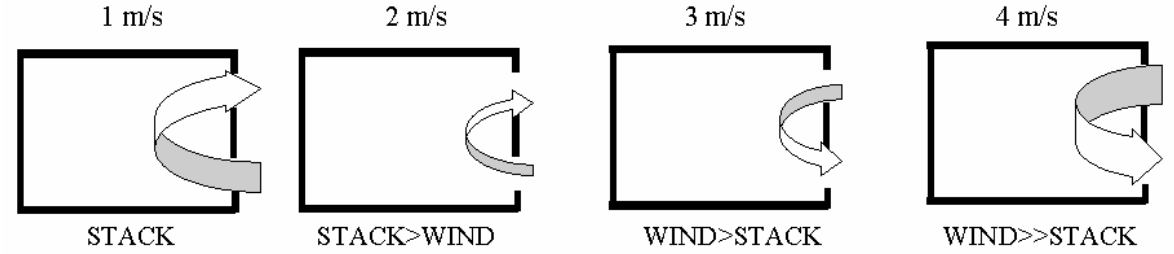

(b)

Fig. 10. The uncertain effects of combined wind and stack forces: (a) reinforcing vs. counteracting effect (b) depiction of counteracting wind and stack effect over a progression of wind speeds.

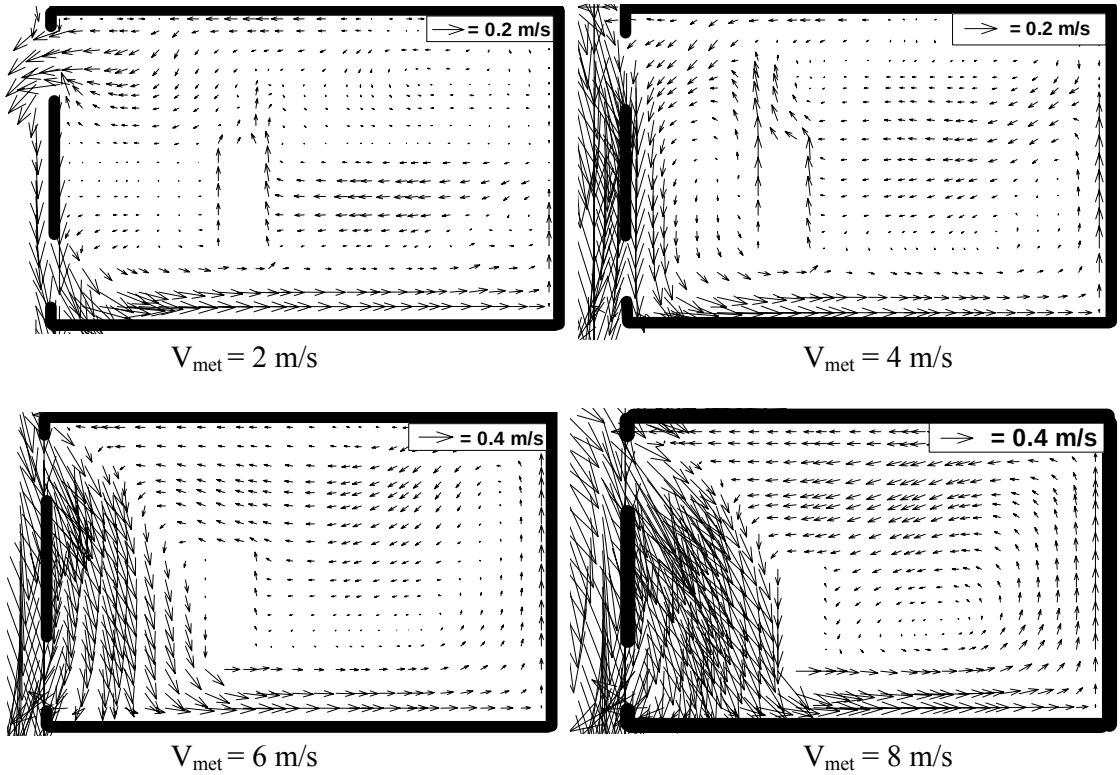

V_{met} = 2 m/s V_{met} = 4 m/s

V_{met} = 6 m/s V_{met} = 8 m/s

Fig. 11. The velocity vectors predicted by CFD to illustrate the counteracting wind and stack effect in the middle level room over a progression of wind speeds, for upper/lower window geometry.